# Paramagnetic Rim Lesions are Specific to Multiple Sclerosis: An International Multicenter 3T MRI Study

Pietro Maggi, MD, PhD,[1,2,3] Pascal Sati, PhD,[4,5] Govind Nair, PhD,[4] Irene C. M. Cortese, MD,[4] Steven Jacobson, PhD,[4] Bryan R. Smith, MD,[4] Avindra Nath, MD,[4] Joan Ohayon, CRNP,[4] Vincent van Pesch, MD, PhD,[1] Gaetano Perrotta, MD,[2] Caroline Pot, MD, PhD,[3] Marie Théaudin, MD,[3] Vittorio Martinelli, MD,[6] Roberta Scotti, MD,[7] Tianxia Wu, PhD,[8] Renaud Du Pasquier, MD,[3] Peter A. Calabresi, MD,[9] Massimo Filippi, MD,[6] Daniel S. Reich, MD, PhD,[4] and Martina Absinta, MD, PhD[9]

In multiple sclerosis (MS), a subset of chronic active white matter lesions are identifiable on magnetic resonance imaging by their paramagnetic rims, and increasing evidence supports their association with severity of clinical disease. We studied their potential role in differential diagnosis, screening an international multicenter clinical research-based sample of 438 individuals affected by different neurological conditions (MS, other inflammatory, infectious, and non-inflammatory conditions). Paramagnetic rim lesions, rare in other neurological conditions (52% of MS vs 7% of non-MS cases), yielded high specificity (93%) in differentiating MS from non-MS. Future prospective multicenter studies should validate their role as a diagnostic biomarker.

ANN NEUROL 2020;88:1034–1042

## Introduction

Improving diagnostic accuracy is a major clinical need in multiple sclerosis (MS).[1] This is especially crucial in the current therapeutic era, when some treatments are highly immunosuppressive and potentially associated with substantial morbidity. In an effort to reduce misdiagnosis, which might be ~20%,[2,3] the discovery of new and pathologically specific imaging biomarkers has garnered renewed attention. Two such markers have been identified on susceptibility-based magnetic resonance imaging (MRI) at 7 and 3T in recent years: the central vein sign (CVS) and paramagnetic rim lesions (PRLs) (Fig 1A). The specificity of the CVS[4–7] arises as a result of tissue remodeling after disruption of the blood–brain barrier in postcapillary venules at the time of lesion onset,[8] whereas PRLs reflect perilesional chronic inflammation, in particular residual and detrimental iron-laden microglia/macrophage accumulation at the lesion edge after acute inflammation subsides (Fig 1B).[9,10] Consistent with neuropathological findings,[11,12] we recently reported a high prevalence of PRLs in MS (>50% of MS cases harbor ≥1 PRL), in addition to an association with clinical disability.[13] However, unlike the CVS, little is known about whether the PRL is specific to MS.

Here, we carried out a retrospective evaluation of the prevalence and MS specificity of PRLs on 3T susceptibility-based magnetic resonance (MR) images in MS ($n$ = 329) versus non-MS cases ($n$ = 83) in a multicenter sample drawn from 5 academic research hospitals at sites in Europe and the USA. We report the prevalence of PRLs in the largest multicenter MS cohort to date, in addition to the diagnostic specificity of the PRL (alone and in combination with the CVS) in MS versus non-MS neurological diseases (both inflammatory and non-inflammatory) and neurotropic viral infections.

## Patients and Methods

From 2013 to early 2020, imaging, laboratory, and clinical data were prospectively collected under institutional

From the [1]Department of Neurology, Cliniques Universitaires Saint-Luc, Université Catholique de Louvain, Brussels, Belgium; [2]Department of Neurology, Hôpital Erasme, Université Libre de Bruxelles, Brussels, Belgium; [3]Service of Neurology, Department of Clinical Neurosciences, Lausanne University Hospital and University of Lausanne, Lausanne, Switzerland; [4]Division of Neuroimmunology and Neurovirology, National Institute of Neurological Disorders and Stroke (NINDS), National Institutes of Health (NIH), Bethesda, MD; [5]Department of Neurology, Cedars-Sinai Medical Center, Los Angeles, CA; [6]Departments of Neurology and Neurophysiology and Neuroimaging Research Unit, Ospedale San Raffaele and Università Vita e Salute, Milan, Italy; [7]Department of Neuroradiology, Ospedale San Raffaele and Università Vita e Salute, Milan, Italy; [8]Clinical Trials Unit, National Institute of Neurological Disorders and Stroke (NINDS), National Institutes of Health (NIH), Bethesda, MD; and [9]Department of Neurology, Johns Hopkins University, Baltimore, MD

Address correspondence to Dr Martina Absinta, Johns Hopkins University, 600 North Wolfe Street, Baltimore, MD 21287. E-mail: mabsint1@jhmi.edu

Additional supporting information can be found in the online version of this article.

Received May 28, 2020, and in revised form Aug 12, 2020. Accepted for publication Aug 13, 2020.

View this article online at wileyonlinelibrary.com. DOI: 10.1002/ana.25877.

 © 2020 American Neurological Association

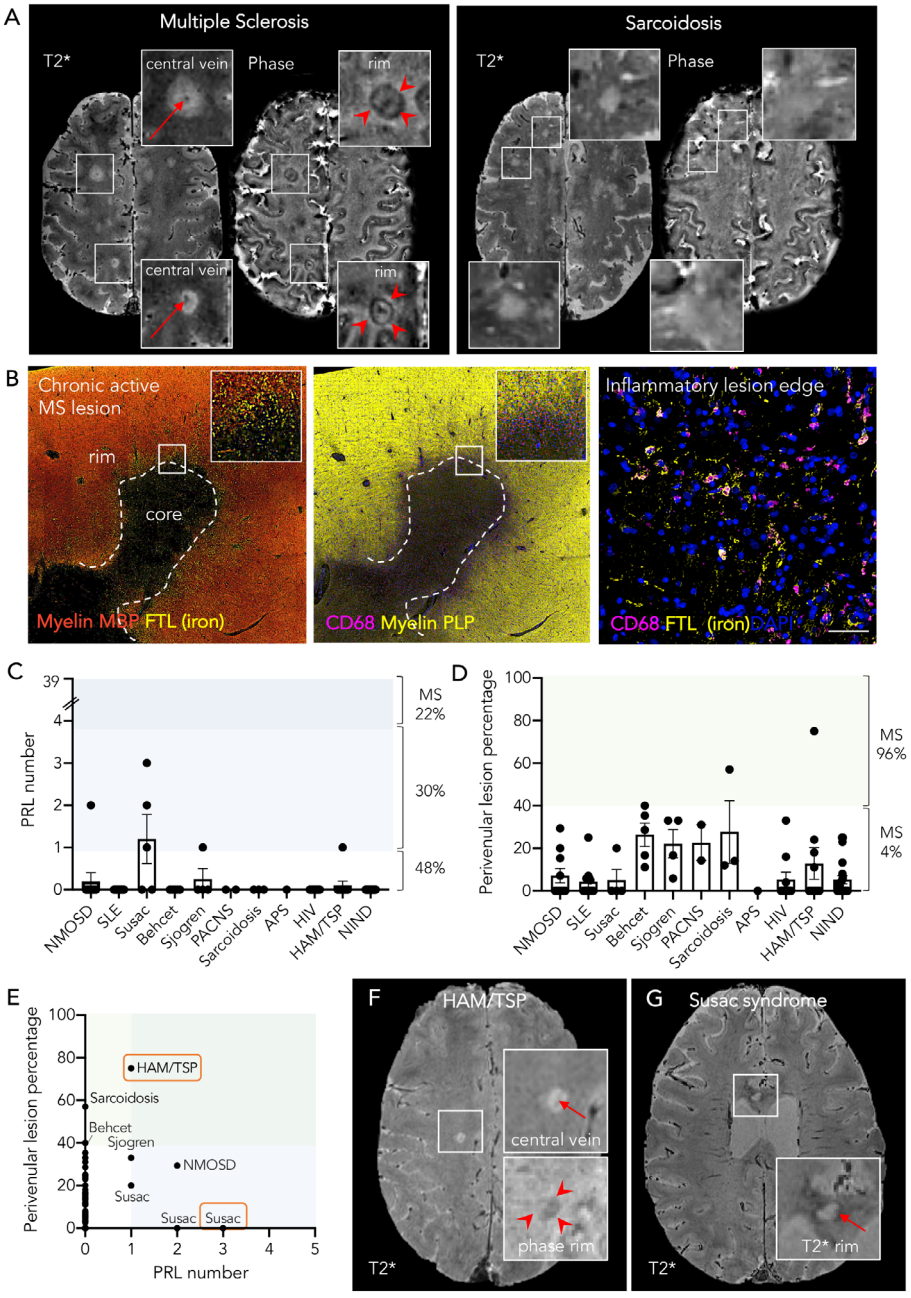


FIGURE 1: (A) Typical susceptibility-based MRI features of MS versus non-MS lesions. Representative axial T2* magnitude and phase 3T MR images from individuals with relapsing–remitting MS and sarcoidosis. The MS lesions are generally centered around veins (arrows) and have a hypointense paramagnetic rim (arrowhead), whereas these features are not typical of non-MS lesions. (B) Representative histopathology of a chronic active rim MS lesion. Fluorescent immunostaining of a chronic active lesion in a 58-year-old man with secondary progressive MS (31 years of disease; autopsy performed as part of a research program). A dense inflammatory infiltrate of iron-laden (FTL) microglia/macrophages (CD68) characterizes the edge of chronic active/rim lesions in MS and is visible as a paramagnetic rim on susceptibility-based MRI. Chronic active/rim lesions are completely demyelinated and without signs of remyelination, as seen with both MBP and PLP myelin staining. Scale bar = 50 µm. (C–G) Frequency of paramagnetic rim lesions and perivenular lesions in non-MS cases. (C, D) Distribution of the frequency of PRL in C and perivenular lesions in D in the 83 non-MS cases enrolled in the study. Overlapping colored regions refer to the frequency of the same MRI variable in the MS cohort. (E) Identification of cases with ≥1 PRL and ≥40% perivenular lesions. Only a single case of HAM/TSP satisfied both criteria (MR images are shown in F), and this might be an individual with both diagnoses. (F) Susceptibility-based MR images of a 49-year-old woman with HAM/TSP, disease duration 10 years, who required 2 walking aids to walk ~20 m without resting. In the inset, 3 of her 4 supratentorial lesions show some MS-like features, including the central vein sign on T2* magnitude images and/or a PRL on phase images. (G) Axial MR images of a 36-year-old man with Susac disease (cases highlighted in C), showing a lesion within the corpus callosum with a rim on T2* images. APS = antiphospholipid syndrome; FTL = ferritin; HAM/TSP = HTLV-associated myelopathy/tropical spastic paraparesis; HIV = human immunodeficiency virus; MBP = myelin basic protein; MR = magnetic resonance; MRI = magnetic resonance imaging; MS = multiple sclerosis; NIND = non-inflammatory neurological diseases; NMOSD = neuromyelitis optica spectrum disorder; PACNS = primary angiitis of the central nervous system; PLP = myelin proteolipid protein; PRL = paramagnetic rim lesions; SLE = systemic lupus erythematosus.

review board-approved protocols in 438 adult individuals with clinical/MRI evidence of central nervous system (CNS) involvement from 5 academic research hospitals: the NIH Clinical Center (Bethesda, MD), Johns Hopkins University Hospital (Baltimore, MD), San Raffaele Hospital (Milan, Italy), Erasme University Hospital and Saint Luc University Hospital (Brussels, Belgium), and Lausanne University Hospital (Lausanne, Switzerland). The study received approval from an ethical standards committee on human experimentation in each of the five academic research hospitals, and written informed consent was obtained from all participants.

Patient eligibility criteria encompassed: (1) age ≥ 18 years, (2) clinical/MRI evidence of CNS involvement and availability of a clinical diagnosis, and (3) availability of 3T 3-dimensional (3D) segmented T2*-weighted echo-planar imaging (EPI) brain images. Cases with diffuse leukoencephalopathy or with no discrete brain lesions were excluded from the analysis a priori. The CONSORT flowchart is shown in Fig 2.

### *MRI Acquisition*

MRI studies were performed on 7 MRI 3T scanners: 4 Philips Intera or Ingenia scanners (Philips Medical Systems, The Netherlands) and 3 Siemens Skyra or Prisma scanners (Siemens AG, Germany). In all scans, 3D T2-Fluid Attenuated Inversion Recovery (T2-FLAIR) images and submillimeter isotropic 3D segmented T2*-weighted EPI,[14–16] providing both magnitude and phase images, were acquired before or during intravenous injection of a single dose (0.1mmol/kg) of gadolinium-based contrast material. The same 3D T2*-EPI sequence[14–16] was adapted and optimized to the different MRI scanners with minimal parameter modification (Supplementary Table S1). Additional routine MRI images were acquired for clinical use, including postcontrast T1-weighted sequences.

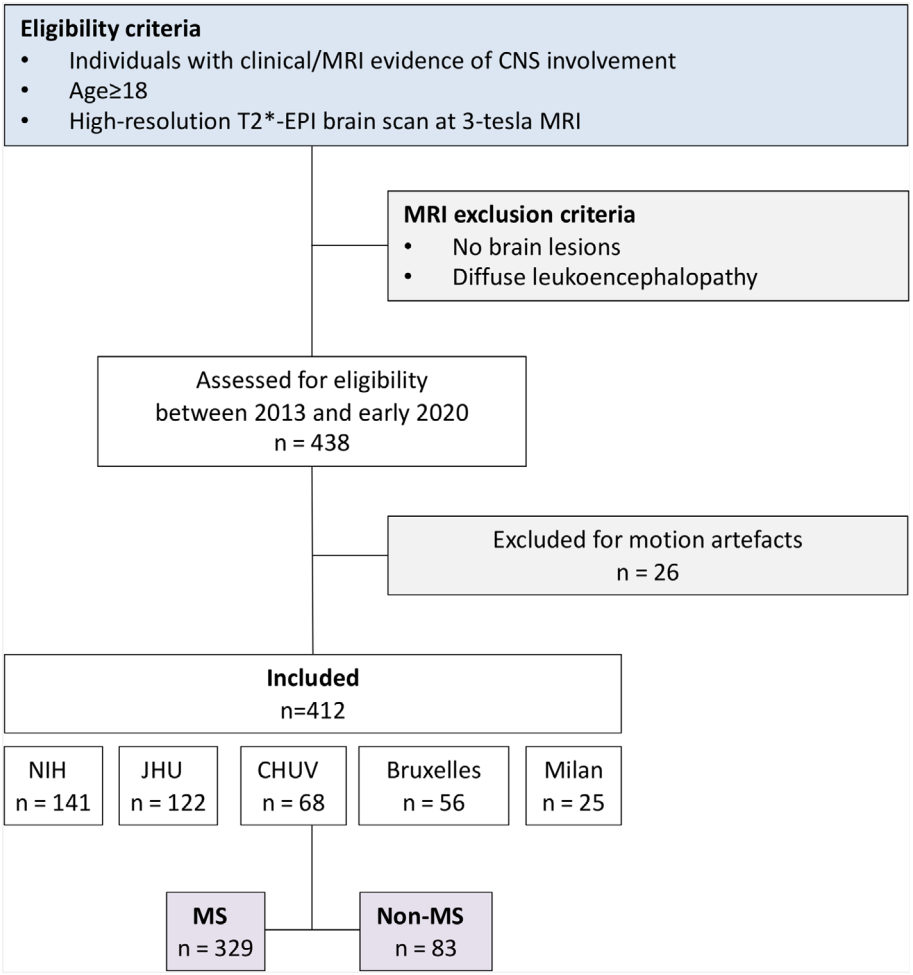


**FIGURE 2: Flow chart summarizing patients' progress through the study. Bruxelles = Erasme University Hospital and Saint Luc University Hospital (Brussels, Belgium); CHUV = Lausanne University Hospital (Lausanne, Switzerland); CNS = central nervous system; EPI = echo-planar imaging; JHU = Johns Hopkins University Hospital (Baltimore, MD); Milan = San Raffaele University Hospital (Milan, Italy); MRI = magnetic resonance imaging; MS = multiple sclerosis; NIH = National Institutes of Health, Clinical Center (Bethesda, MD). [Color figure can be viewed at www.annalsofneurology.org]**

### PRL and CVS Assessment

Given that raters were partially involved in the recruitment of cases (P.M. for the European cases; M.A. and D.S.R. for the US cases), all images were de-identified before analysis, including the final diagnosis. In each individual, the number of supratentorial chronic non-enhancing PRLs on unwrapped phase images was determined by consensus of 2 raters (P.M. and M.A.). Inter-rater reliability was tested for all non-MS cases and an equal number of MS cases. All non-MS cases with PRLs were reviewed further by a third rater (D.S.R.) for final adjudication. A chronic lesion was defined as a PRL when it showed a hypointense rim on phase images and internal isointensity to extralesional white matter.[17] In order to compare the results of this large multicenter MS cohort with our previously published work (single-center study),[13] MS cases were classified further based on the number of PRLs into 3 groups (0, 1–3, and ≥4 PRLs, respectively), as previously described.[13]

For all non-MS cases and an equal number of randomly selected MS cases, the percentage of CVS lesions was also assessed by consensus of 2 raters (P.M. and M.A.), according to the North American Imaging in Multiple Sclerosis (NAIMS) Cooperative guidelines,[18] as previously described.[6] In detail, all cases were divided equally between the two raters (P.M. and M.A.) for initial CVS assessment, then each rater reviewed the CVS annotations of the other rater for consensus and final agreement. Inter-rater reliability was assessed based on the previously described "40% rule."[4,6,19]

### Statistical Analysis

Demographic, clinical, and MRI differences were assessed with ANOVA and Tukey's post-hoc multiple-comparison test, with Fisher's exact or chi-square test, when appropriate. The inter-rater reliability for PRL and CVS assessment was computed using Cohen's κ. The association of the number of PRLs with disability and disease severity scores (Expanded Disability Status Scale [EDSS],[20] MS severity score [MSSS],[21] and global age-related MS severity score [ARMSS][22]) was evaluated using Spearman correlation coefficients, because the number of PRLs had a highly skewed distribution (skewness = 4.4) and sex, age, and disease duration had no significant effect on the number of PRLs. Clinical phenotype was not considered as a covariate because it was significantly correlated ($p < 0.0001$) with EDSS, MSSS, and ARMSS.

The SAS procedure LOGISTIC was used to produce receiver operating characteristic (ROC) curves. In the logistic regression model, diagnosis (MS vs non-MS) was a dependent variable and PRL (or CVS) an independent variable. The ROC curve is a plot of sensitivity against 1 − specificity. The sensitivity and specificity values were obtained by varying the cut-off to dichotomize PRL (or CVS). Youden's index method was used to obtain the optimal cut-off value for each biomarker.

## Results

Of 438 consecutive eligible cases, data from 412 were included in this analysis (26 were excluded for motion-related MRI artifacts) and grouped according to their clinical diagnosis (based on international published diagnostic criteria), as follows. There were 329 individuals with MS diagnosed according to the 2017 McDonald criteria[23,24] (7 with clinically isolated syndrome, 226 relapsing–remitting, and 96 progressive). There were 41 individuals with other inflammatory neurological diseases (OIND), including: 11 cases of neuromyelitis optica spectrum disorder (NMOSD[25]; 9 of them were AQP4 antibody-positive, 1 MOG antibody-positive, and 1 seronegative); 10 cases of systemic lupus erythematosus (SLE)[26]; 5 cases of Susac syndrome[27]; 5 cases of Behçet disease[28]; 4 cases of Sjögren disease[29]; 3 cases of sarcoidosis[30]; 2 cases of primary angiitis of the central nervous system (PACNS, imaging or biopsy proven)[31]; and 1 case of antiphospholipid syndrome (APS).[32] There were 20 individuals infected by neurotropic viruses, randomly selected from larger datasets, including 10 individuals with human T-lymphotropic virus (HTLV)-associated myelopathy/tropical spastic paraparesis (HAM/TSP) and 10 individuals with HIV infection, without other comorbidities, on antiretroviral therapy. There were 22 individuals affected by non-inflammatory neurological diseases (NINDs), including small vessel disease and migraine. Demographic and clinical data are reported in Table 1. The inter-rater reliability for PRL and CVS assessment were "substantial/good," with Cohen's κ of 0.79 and 0.86, respectively.

In the 412 scans analyzed, PRLs were detected in 172 of 329 MS cases (52%) versus 6 of 83 non-MS cases (7%). In MS, 58% of progressive cases had ≥1 PRL, compared with 50% of relapsing cases. The number of PRLs was positively correlated with all disability and severity scores (EDSS Spearman $r = 0.17$, $p = 0.002$; MSSS $r = 0.18$, $p = 0.001$; and global ARMSS $r = 0.22$, $p < 0.0001$). When previously published PRL categories were implemented,[13] cases with ≥4 PRLs had higher disability and severity scores, but not significantly longer disease duration or older age (Table 2). In addition, they were 1.8-fold more frequently treated with second-line antibody-based therapies than those without PRLs ($\chi^2$ $p = 0.0002$).

In non-MS cases, PRLs were seen in only a few other inflammatory/infectious neurological conditions (Table 1; Fig 1C–G). The highest prevalence of PRLs was

**TABLE 1. Cohort Characteristics**

| Characteristic | OIND | NIND | Neurotropic Viruses: HTLV-Infected HAM/TSP | Neurotropic Viruses: HIV-Infected | MS |
|---|---|---|---|---|---|
| Participants, n | 41 | 22 | 10 | 10 | 329 |
| Women, n (%) | 30 (73%) | 16 (73%) | 7 (70%) | 1 (10%) | 198 (60%) |
| Age, mean (range), yr | 45 (21–74) | 51 (26–75) | 57 (37–75) | 56 (45–62) | 45 (20–76) |
| OCB positive of cases with CSF available for review, n (%) | 10/32 (31%) | 0/5 (0%) | 9/9 (100%) | — | 121/151 (80%) |
| **Fulfillment of dissemination in space MRI criteria according to McDonald revised MS criteria 2017** | | | | | |
| Cases, n (%) | 26/41 (63%) | 6/22 (27%) | 2/10 (20%) | 0/10 (0%) | 329/329 (100%) |
| **Paramagnetic rim lesion detection** | | | | | |
| Cases with ≥1 PRL, n (%) | 5 (12%) | 0 | 1 (10%) | 0 | All: 172/329 (52%) CIS/RR: 116/233 (50%) Progressive: 56/96 (58%) |
| **Perivenular lesion detection** | | | | | |
| Perivenular lesion frequency, mean (range) | 12.4% (0–57%) | 5.3% (0–25%) | 12.8% (0–75%) | 5.3% (0–33%) | 75.2% (35–100%) |
| Cases with ≥40% perivenular lesions,[a] n (%) | 2 (5%) | 0 | 1 (10%) | 0 | 80/83 (96%) |

[a]Cases were dichotomized as overall CVS-positive versus CVS-negative based on the previously described "40% rule"[4,6,19].

CIS = clinically isolated syndrome; CVS = central vein sign; HAM/TSP = HTLV-associated myelopathy/tropical spastic paraparesis; HIV = human immunodeficiency virus; HTLV = human T-lymphotropic virus; MRI = magnetic resonance imaging; MS = multiple sclerosis; NIND = non-inflammatory neurological diseases; OCB = oligoclonal bands; OIND = other inflammatory/infectious neurological diseases; PRL = paramagnetic rim lesion; RR = relapsing–remitting.

detected in Susac syndrome (3 of 5 cases, 60%). Of these, 1 case had 3 PRLs, 1 had 2 PRLs, and 1 had 1 PRL. These were located within the corpus callosum and had a signal intensity isointense to cerebrospinal fluid on T1-weighted images, suggesting severe tissue damage (Fig 1G). Sporadically, PRLs were seen also in NMOSD (1 AQP4-positive case with 2 PRLs), Sjögren disease (1 case with 1 PRL), and HAM/TSP (1 case with 1 PRL; Fig 1F). None of the NIND (including small vessel disease and migraine) or HIV cases had PRLs.

Consistent with previous data in the literature,[4,6,7] the frequency of CVS lesions was remarkably high in our MS cohort (mean 75%, median 75%, range 35–100%) and was unrelated to the number of PRLs (Table 1). In contrast, non-MS cases showed very low CVS lesion frequency (mean 9%, median 0%, range 0–75%). Among non-MS cases, HAM/TSP and OIND showed the highest mean frequency of CVS lesions (13% and 12%, respectively), followed by HIV (5%), and NIND (5%) (Table 1; Fig 1D).

Of relevance, 34 of 83 (41%) non-MS cases fulfilled the dissemination in space (DIS) MRI criteria for MS, according to the 2017 revised McDonald criteria.[24] In this context, the identification of ≥1 PRL (optimal cut-off) was associated with high diagnostic specificity (93%, 95% confidence interval [CI] = 85–87%), but relatively low sensitivity (52%, 95% CI = 47–58%) and overall accuracy (area under ROC curve = 0.77, 95% CI = 0.71–0.83), whereas CVS detection alone (optimal cut-off 35.5–38%) could better discriminate MS from non-MS cases with

**TABLE 2. Multiple Sclerosis Cohort Characteristics by Paramagnetic Rim Lesion Category**

| PRL category | No detected PRL | 1–3 PRLs | ≥4 PRLs | Statistical Analysis |
|---|---|---|---|---|
| n (%) | 157 (48%) | 99 (30%) | 73 (22%) | — |
| **Demographic and clinical characteristics** | | | | |
| Clinical phenotype, n (%) | CIS/RR 117 (74%) | CIS/RR 72 (73%) | RR 44 (60%) | Fisher 2 × 3 $p$ = 0.057 n.s. |
| | SP 28 (18%) | SP 19 (19%) | SP 13 (18%) | |
| | PP 12 (8%) | PP 8 (8%) | PP 16 (22%) | |
| Sex (female), n (%) | 101 (64%) | 57 (58%) | 40 (55%) | Fisher 2 × 3 $p$ = 0.4 n.s. |
| Age, mean (SD), yr | 46.3 (13.0) | 44.1 (1124) | 44.0 (12.6) | ANOVA $p$ = 0.3 n.s. |
| Disease duration, mean (SD), yr | 12.1 (10) | 11.1 (10) | 11.2 (8) | ANOVA $p$ = 0.6 n.s. |
| EDSS, median (range) | 2 (0–8)[a] | 2 (0–8) | 3 (0–7.5)[a] | ANOVA $p$ = 0.006 |
| MSSS, mean (SD) | 3.3 (2.5) [a] | 3.8 (2.5) | 4.7 (3.0)[a] | ANOVA $p$ = 0.001 |
| Global ARMSS, mean (SD) | 3.7 (2.4)[b] | 4.3 (2.6)[a] | 5.3 (2.5)[ab] | ANOVA $p$ < 0.0001 |
| **Treatment,[c] % cases** | | | | |
| Untreated | 30% | 33% | 19% | $\chi^2$ $p$ = 0.002[d] |
| First-line injectables | 27% | 27% | 19% | |
| Oral | 22% | 28% | 22% | |
| Antibody-based | 22% | 13% | 40% | |
| **Perivenular lesion detection[e]** | | | | |
| Perivenular lesion percentage, mean (range) | 75% (35–100%) | 77% (38–100%) | 74% (57–92%) | ANOVA $p$ = 0.7 n.s. |
| Cases with <40% perivenular lesions, n (%) | 2/33 (6%) | 1/30 (3%) | 0/20 (0%) | — |

[a] $p < 0.05$ , Turkey's post-hoc multiple-comparison test.
[b] $p < 0.0001$, Tukey's post-hoc multiple-comparison test.
[c] Type of treatments: first-line injectables (interferon beta, glatiramer acetate); oral (fingolimod, dimethyl fumarate, teriflunomide), antibody based (natalizumab, rituximab, ocrelizumab, alemtuzumab).
[d] Refers to antibody-based treatments versus all other types of treatments (table 2 × 3, d.f. = 2).
[e] The perivenular lesion detection was assessed in 83 randomly selected MS cases with ≥3 qualifying brain lesions according to the NAIMS CVS detection guidelines.[18]
ARMSS = Age Related Multiple Sclerosis Severity[22]; CIS = clinically isolated syndrome; CVS = central vein sign; EDSS = Expanded Disability Status Scale[20]; MS = multiple sclerosis; MSSS = MS severity score[21]; NAIMS = North American Imaging in Multiple Sclerosis (NAIMS) Cooperative; n.s. = not significant; PP = primary progressive; PRL = paramagnetic rim lesion; RR = relapsing–remitting; SD = standard deviation; SP = secondary progressive.

high specificity (96%, 95% CI = 89–99%), sensitivity (99%, 95% CI = 93–100%), and accuracy (area under ROC curve = 0.99, 95% CI = 0.98–1). The optimal cut-off for CVS (35.5–38%) is in line with the previously reported "40% rule".[4,6,19] The combination of the two biomarkers (fulfillment of both ≥1 PRL and ≥40% CVS)

further improved the specificity (99%), but sensitivity remained low (59%). In the subset of non-MS cases with OCB available to review (n = 46), no case fully satisfied all 4 criteria (DIS, OCB positivity, CVS >35.5–38%, and PRL ≥1).

## Discussion

In this cross-sectional study, we evaluated the prevalence and specificity of PRLs on 3T susceptibility-based images, screening a multicenter academic clinical research-based sample of individuals affected by a variety of neurological conditions. Unlike findings in MS, we found that PRLs were observed only rarely in inflammatory/infectious neurological conditions. Furthermore, the absence of PRLs in individuals without underlying inflammatory neurological disease provides additional support to the recent notion that PRLs in MS indicate perilesional chronic inflammation.[9,10]

This 3T study expands on preliminary results from 2 previous 7T[33,34] studies and one 3T[35] study in limited non-MS cohorts. In OIND, the highest prevalence of PRLs was observed in Susac syndrome, a rare autoimmune disease causing the occlusion of small vessels of the brain, retina, and inner ear.[36] In line with its etiopathogenesis, MRI features of corpus callosum lesions in Susac syndrome (CSF-like T1 signal, T2* rim, and no central veins) resemble those seen in lacunar ischemic lesions.[33] We can speculate that the origin of the iron in Susac syndrome's PRLs might not be related to perilesional chronic inflammation (accumulation of iron-laden microglia/macrophages), as occurs in MS, but to sequelae of the hemoglobin extravasation (heme-iron bioproducts) at the edge of the post-ischemic cavitation. In addition, we had 1 HAM/TSP case that was an outlier, containing both a high proportion (75%) of CVS lesions and a PRL indistinguishable from those seen in the MS cohort; this individual also met 2017 McDonald criteria for dissemination in space, and we speculate that both MS and HAM/TSP were present simultaneously (Fig 1F). Aside from these cases, very few non-MS cases, including the relatively frequent NMOSD, had PRLs.

Thus, the detection of PRLs might prove a valuable tool in the differential diagnostic work-up, especially for improving diagnostic specificity. Although the overall diagnostic performance of PRL detection alone is inferior to the CVS, particularly with respect to sensitivity, our data suggest that the combination of these two imaging biomarkers might help in the diagnostic work-up in two specific scenarios: (1) cases with suspected MS but low frequency of CVS (eg, owing to small vessel disease comorbidity);[4,37,38] and (2) cases with suspected non-MS but a high frequency of CVS lesions.[6,19]

The results of this study also strengthen our recently published single-center MRI data on the frequency of PRLs and their association with disability in MS,[13] expanding the results to what is, to date, the largest multicenter cohort of MS cases acquired with the same 3T susceptibility-based sequence. We confirm that more than half of MS cases (52%) harbor chronically inflamed lesions despite receiving approved disease-modifying treatments specifically designed to be highly effective in reducing T- and/or B-lymphocyte-driven inflammation. We also replicated that a higher PRL burden can stratify MS cases with significantly higher disability (as assessed by the EDSS)[20] and MS severity (accounting for the disease duration [MSSS][21] or for patient age [global ARMSS][22]). Given that some PRLs might fade over time,[39] this further corroborates the role of PRL accrual in potentially driving clinical progression at a young age and/or relatively short disease duration.[13,40]

A major technical advantage of this large multicenter study (438 eligible individuals) is the use of the same 3T EPI MRI sequence,[14,15] with minimal parameter adjustments across MS centers and centralized analysis. The high-resolution susceptibility-based sequence implemented here has been shown to provide T2*/FLAIR*[14,15] and phase images for reliable assessment of both CVS[6,19] and PRLs.[16] The short acquisition time (~5 minutes) makes this sequence compatible with routine clinical scanning.

This work has some limitations, including its retrospective nature and use of a convenience sample (with a relatively low number of non-MS cases in comparison to MS cases and skewness toward relapsing cases [70% of all MS]). Also, it might not reflect real-world diagnosis in a newly presenting population. Although clinical implementation of these diagnostic biomarkers might be limited by the availability of 3T MR scanners, the preference for gadolinium injection to increase the sensitivity of CVS detection (but not necessarily of PRL detection), the current need for manual assessment of CVS and PRLs (although automatic detection algorithms[41,42] are being developed), and the lack of a product 3D T2*-EPI sequence on several scanner platforms, it is not difficult to envision these barriers being overcome.

In conclusion, PRLs yielded high specificity for MS lesions. Future prospective multicenter studies should further validate their role as a diagnostic biomarker.

## Acknowledgments

The study was partially supported by Intramural Research Program of the NIH/NINDS (to D.S.R.), by NIH/NINDS (grant R01NS082347, to P.A.C.), and by the Conrad N. Hilton Foundation (grant 17313, to M.A.).

We thank the study participants; the neuroimmunology clinics in each center for recruiting and evaluating the patients and for coordinating the scans; and Blake Dewey, Antonella Iadanza, Tobias Kober, Julie Absil, and Jean-Baptiste Ledoux for assistance with 3T MRI scan acquisition. We thank Dragan Maric for helping with the fluorescent multiplex immunostaining of brain MS autopsy tissue (shown in Fig 1).

## Author Contributions

P.M., D.S.R., and M.A. contributed to the conception and design of the study; P.M., P.S., G.N., V.M., R.S., G.P., V.V.P., B.R.S., A.N., S.J., T.W., J.O., I.C.M.C., C.P., M.T., R.D.P., T.W., P.A.C., M.F., D.S.R., and M.A. contributed to the acquisition and analysis of data; P.M., D.S.R., and M.A. contributed to drafting the text and preparing the figures.

## Potential Conflict of Interest

Nothing to report.

## References

1. Solomon AJ, Corboy JR. The tension between early diagnosis and misdiagnosis of multiple sclerosis. Nat Rev Neurol 2017;13:567–572.
2. Solomon AJ, Bourdette DN, Cross AH, et al. The contemporary spectrum of multiple sclerosis misdiagnosis: a multicenter study. Neurology 2016;87:1393–1399.
3. Kaisey M, Solomon AJ, Luu M, et al. Incidence of multiple sclerosis misdiagnosis in referrals to two academic centers. Mult Scler Relat Disord 2019;30:51–56.
4. Tallantyre EC, Dixon JE, Donaldson I, et al. Ultra-high-field imaging distinguishes MS lesions from asymptomatic white matter lesions. Neurology 2011;76:534–539.
5. Mistry N, Dixon J, Tallantyre E, et al. Central veins in brain lesions visualized with high-field magnetic resonance imaging: a pathologically specific diagnostic biomarker for inflammatory demyelination in the brain. JAMA Neurol 2013;70:623–628.
6. Maggi P, Absinta M, Grammatico M, et al. Central vein sign differentiates multiple sclerosis from central nervous system inflammatory vasculopathies. Ann Neurol 2018;83:283–294.
7. Sinnecker T, Clarke MA, Meier D, et al. Evaluation of the central vein sign as a diagnostic imaging biomarker in multiple sclerosis. JAMA Neurol 2019;76:1446.
8. Absinta M, Nair G, Monaco MCG, et al. The "central vein sign" in inflammatory demyelination: the role of fibrillar collagen type I. Ann Neurol 2019;85:934–942.
9. Absinta M, Sati P, Schindler M, et al. Persistent 7-tesla phase rim predicts poor outcome in new multiple sclerosis patient lesions. J Clin Invest 2016;126:2597–2609.
10. Dal-Bianco A, Grabner G, Kronnerwetter C, et al. Slow expansion of multiple sclerosis iron rim lesions: pathology and 7 T magnetic resonance imaging. Acta Neuropathol 2017;133:25–42.
11. Frischer JM, Weigand SD, Guo Y, et al. Clinical and pathological insights into the dynamic nature of the white matter multiple sclerosis plaque. Ann Neurol 2015;78:710–721.
12. Luchetti S, Fransen NL, van Eden CG, et al. Progressive multiple sclerosis patients show substantial lesion activity that correlates with clinical disease severity and sex: a retrospective autopsy cohort analysis. Acta Neuropathol 2018;135:511–528.
13. Absinta M, Sati P, Masuzzo F, et al. Association of Chronic Active Multiple Sclerosis Lesions with Disability in Vivo. JAMA Neurol 2019;76:1520.
14. Sati P, George IC, Shea CD, et al. FLAIR*: a combined MR contrast technique for visualizing white matter lesions and parenchymal veins. Radiology 2012;265:926–932.
15. Sati P, Thomasson DM, Li N, et al. Rapid, high-resolution, whole-brain, susceptibility-based MRI of multiple sclerosis. Mult Scler 2014;20:1464–1470.
16. Absinta M, Sati P, Fechner A, et al. Identification of chronic active multiple sclerosis lesions on 3T MRI. AJNR Am J Neuroradiol 2018;39:1233–1238.
17. Yao B, Bagnato F, Matsuura E, et al. Chronic multiple sclerosis lesions: characterization with high-field-strength MR imaging. Radiology 2012;262:206–215.
18. Sati P, Oh J, Constable RT, et al. The central vein sign and its clinical evaluation for the diagnosis of multiple sclerosis: a consensus statement from the north American imaging in multiple sclerosis cooperative. Nat Rev Neurol 2016;12:714–722.
19. Maggi P, Absinta M, Sati P, et al. The "central vein sign" in patients with diagnostic "red flags" for multiple sclerosis: a prospective multicenter 3T study. Mult Scler 2020;26:421–432.
20. Kurtzke JF. Rating neurologic impairment in multiple sclerosis: an expanded disability status scale (EDSS). Neurology 1983;33:1444–1452.
21. Roxburgh RH, Seaman SR, Masterman T, et al. Multiple sclerosis severity score: using disability and disease duration to rate disease severity. Neurology 2005;64:1144–1151.
22. Manouchehrinia A, Westerlind H, Kingwell E, et al. Age related multiple sclerosis severity score: disability ranked by age. Mult Scler 2017;23:1938–1946.
23. Polman CH, Reingold SC, Banwell B, et al. Diagnostic criteria for multiple sclerosis: 2010 revisions to the McDonald criteria. Ann Neurol 2011;69:292–302.
24. Thompson AJ, Banwell BL, Barkhof F, et al. Diagnosis of multiple sclerosis: 2017 revisions of the McDonald criteria. Lancet Neurol 2018;17:162–173.
25. Wingerchuk DM, Banwell B, Bennett JL, et al. International consensus diagnostic criteria for neuromyelitis optica spectrum disorders. Neurology 2015;85:177–189.
26. Petri M, Orbai AM, Alarcon GS, et al. Derivation and validation of the systemic lupus international collaborating clinics classification criteria for systemic lupus erythematosus. Arthritis Rheum 2012;64:2677–2686.
27. Kleffner I, Dorr J, Ringelstein M, et al. Diagnostic criteria for Susac syndrome. J Neurol Neurosurg Psychiatry 2016;87:1287–1295.
28. Disease ISGfBs. Criteria for diagnosis of Behcet's disease. Lancet 1990;335:1078–1080.
29. Shiboski CH, Shiboski SC, Seror R, et al. American College of Rheumatology/European league against rheumatism classification criteria for primary Sjogren's syndrome: a consensus and data-driven methodology involving three international patient cohorts. Arthritis Rheumatol 2017;69:35–45.
30. Stern BJ, Royal W 3rd, Gelfand JM, et al. Definition and consensus diagnostic criteria for Neurosarcoidosis: from the Neurosarcoidosis consortium consensus group. JAMA Neurol 2018;75:1546–1553.
31. Schuster S, Bachmann H, Thom V, et al. Subtypes of primary angiitis of the CNS identified by MRI patterns reflect the size of affected vessels. J Neurol Neurosurg Psychiatry 2017;88:749–755.

32. Miyakis S, Lockshin MD, Atsumi T, et al. International consensus statement on an update of the classification criteria for definite antiphospholipid syndrome (APS). J Thromb Haemost 2006;4: 295–306.

33. Wuerfel J, Sinnecker T, Ringelstein EB, et al. Lesion morphology at 7 tesla MRI differentiates Susac syndrome from multiple sclerosis. Mult Scler 2012;18:1592–1599.

34. Sinnecker T, Schumacher S, Mueller K, et al. MRI phase changes in multiple sclerosis vs neuromyelitis optica lesions at 7T. Neurol Neuroimmunol Neuroinflamm 2016;3:e259.

35. Clarke MA, Pareto D, Pessini-Ferreira L, et al. Value of 3T susceptibility-weighted imaging in the diagnosis of multiple sclerosis. AJNR Am J Neuroradiol 2020;41:1001–1008.

36. Dorr J, Krautwald S, Wildemann B, et al. Characteristics of Susac syndrome: a review of all reported cases. Nat Rev Neurol 2013;9: 307–316.

37. Mistry N, Abdel-Fahim R, Samaraweera A, et al. Imaging central veins in brain lesions with 3-T T2*-weighted magnetic resonance imaging differentiates multiple sclerosis from microangiopathic brain lesions. Mult Scler 2016;22:1289–1296.

38. Guisset F, Lolli V, Bugli C, et al. The central vein sign in MS patients with vascular comorbidities. Mult Scler 2020. https://doi.org/10.1177/1352458520943785. Online ahead of print. PMID: 32749948.

39. Chen W, Gauthier SA, Gupta A, et al. Quantitative susceptibility mapping of multiple sclerosis lesions at various ages. Radiology 2014;271:183–192.

40. Bozin I, Ge Y, Kuchling J, et al. Magnetic resonance phase alterations in multiple sclerosis patients with short and long disease duration. PLoS One 2015;10:e0128386.

41. Dworkin JD, Sati P, Solomon A, et al. Automated integration of multimodal MRI for the probabilistic detection of the central vein sign in white matter lesions. AJNR Am J Neuroradiol 2018;39:1806–1813.

42. Maggi P, Fartaria MJ, Jorge J, et al. CVSnet: a machine learning approach for automated central vein sign assessment in multiple sclerosis. NMR Biomed 2020;33:e4283.